ELSEVIER

www.elsevier.nl/locate/carres

Carbohydrate Research 326 (2000) 277–294

CARBOHYDRATE RESEARCH

Structural characterization of the pectic polysaccharide rhamnogalacturonan II: evidence for the backbone location of the aceric acid-containing oligoglycosyl side chain

Stéphane Vidal [a,b,*], Thierry Doco [a], Pascale Williams [a], Patrice Pellerin [a], William S. York [c], Malcolm A. O'Neill [c], John Glushka [c], Alan G. Darvill [c], Peter Albersheim [c]

[a] *Institut National de la Recherche Agronomique, Institut des Produits de la Vigne, Unité de Recherches Biopolymères et Arômes, 2 Place Viala, F-34060 Montpellier, France*
[b] *Gist-Brocades France S.A., 15 rue des Comtesses, BP 239, F-59472 Seclin, France*
[c] *Complex Carbohydrate Research Center, The University of Georgia, 220 Riverbend Road, Athens, GA 30602-4712, USA*

Received 12 July 1999; accepted 16 January 2000

Abstract

Monomeric rhamnogalacturonan II (mRG-II) was isolated from red wine and the reducing-end galacturonic acid of the backbone converted to L-galactonic acid by treatment with $NaBH_4$. The resulting product (mRG-II′ol) was treated with a cell-free extract from *Penicillium daleae*, a fungus that has been shown to produce RG-II-fragmenting glycanases. The enzymatically generated products were fractionated by size-exclusion and anion-exchange chromatographies and the quantitatively major oligosaccharide fraction isolated. This fraction contained structurally related oligosaccharides that differed only in the presence or absence of a single Kdo residue. The Kdo residue was removed by acid hydrolysis and the resulting oligosaccharide then characterized by 1- and 2D ^1H NMR spectroscopy, ESMS, and by glycosyl-residue and glycosyl-linkage composition analyses. The results of these analyses provide evidence for the presence of at least two structurally related oligosaccharides in the ratio $\sim$6:1. The backbone of these oligosaccharides is composed of five (1→4)-linked α-D-Gal*p*A residues and a (1→3)-linked L-galactonate. The (1→4)-linked Gal*p*A residue adjacent to the terminal non-reducing Gal*p*A residue of the backbone is substituted at O-2 with an apiosyl-containing side chain. β-L-Ara*f*-(1→5)-β-D-Dha*p*A is likely to be linked to O-3 of the Gal*p*A residue at the non-reducing end of the backbone in the quantitatively major oligosaccharide and to O-3 of a (1→4)-linked Gal*p*A residue in the backbone of the minor oligosaccharide. Furthermore, the results of our studies have shown that the enzymically generated aceryl acid-containing oligosaccharide contains an α-linked aceryl acid residue and a β-linked galactosyl residue. Thus, the anomeric linkages of these residues in RG-II should be revised.

Keywords: Rhamnogalacturonan II; Oligosaccharides; *Penicillium daleae*; Pectin; NMR spectroscopy; Wine; Plant cell wall

1. Introduction

Rhamnogalacturonan-II (RG-II) is a structurally complex pectic polysaccharide that is

* Corresponding author. Tel.: +33-4-99-612585; fax: +33-4-99-612683.
E-mail address: vidals@ensam.inra.fr (S. Vidal)

0008-6215/00/$ - see front matter
PII: S0008-6215(00)00036-7

released, as a low-molecular-weight (5–10 kDa) polysaccharide, by treating plant primary cell walls with *endo*-α-(1→4)-polygalacturonase or with pectinases [1–6]. RG-II is also present in fruit-derived products including wine and juices [4]. RG-II exists in the primary wall and in wine predominantly as a dimer (dRG-II-B) that is covalently linked by a 1:2 borate diol ester [6–8]. The cross-linking of RG-II in the wall is believed to result in the formation of a covalently cross-linked pectic matrix [9,10]. This matrix may be involved in regulating the pore size of primary walls [11] and some of the physical properties of the wall [11,12]. The ability of dRG-II-B to form complexes with selected di- (e.g., Pb^{2+}, Ba^{2+}, and Sr^{2+}) and trivalent (e.g., La^{3+}) cations [7] is believed to account for the low levels of free Pb^{2+} in wine, since most of the Pb^{2+} is complexed with dRG-II-B [13,14]. Recent studies have suggested that dRG-II-B-bound Pb^{2+} is not absorbed through the gastro-intestinal tract and may therefore reduce the risk of chronic lead poisoning [15]. The borate ester cross-linked RG-II dimer isolated from the medicinal herb *Panax Ginseng* has been reported to enhance the expression of the macrophage Fc receptor [16].

The backbone of RG-II contains at least eight (1→4)-linked α-D-galactopyranosyluronic acid residues. Four structurally distinct oligoglycosyl side chains (A–D in Fig. 1) are attached to the backbone [17–21]. These side chains have been structurally characterized, but their distribution on the backbone has not been determined. The selective cleavage of per-O-methylated RG-II has provided evidence that the Api*f* and Dha residues are directly attached the backbone [22]. The distribution of the oligoglycosyl side chains on the RG-II backbone has recently been examined by 2D NMR spectroscopy and has led to the

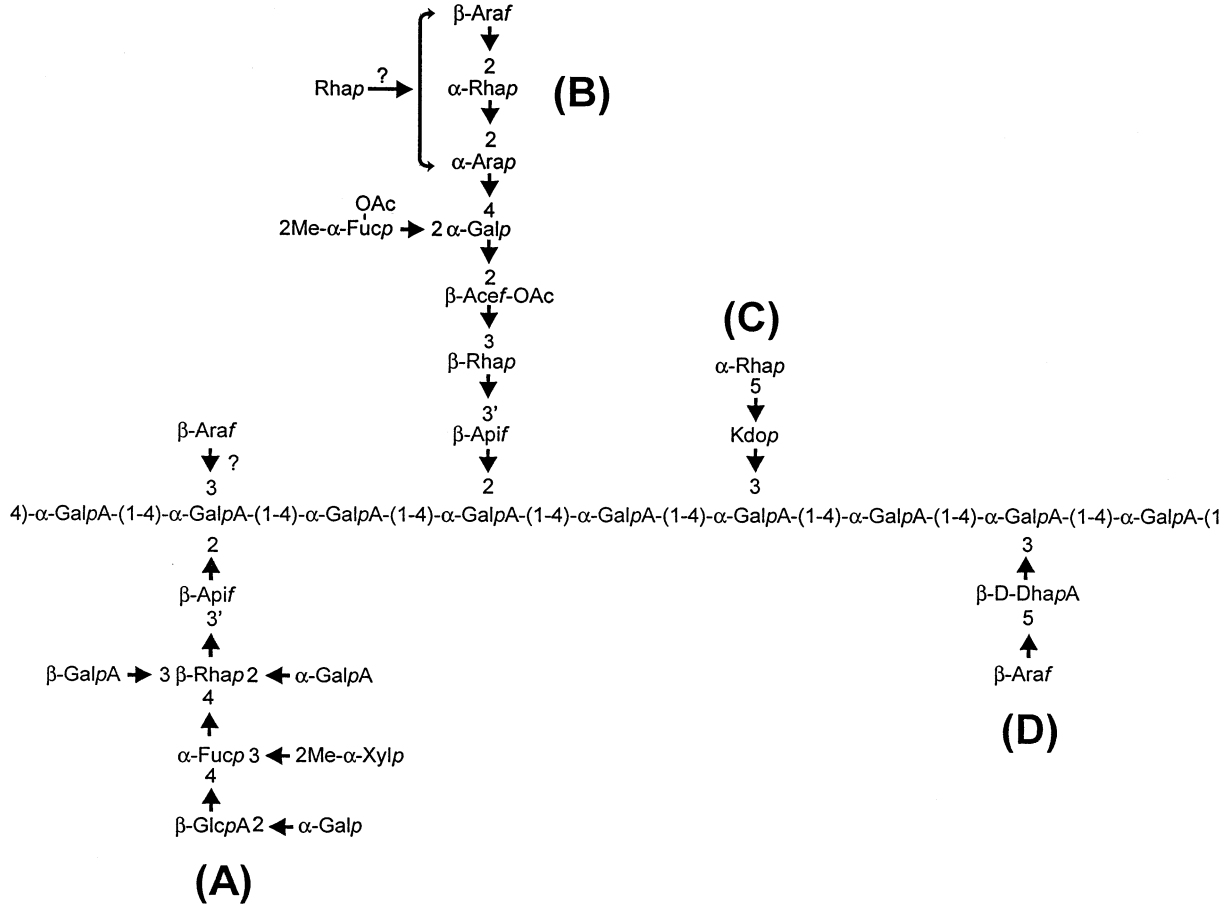

Fig. 1. The glycosyl sequence of RG-II. The (1→4)-linked α-D-Gal*p*A backbone of RG-II is substituted with four structurally different oligoglycosyl side chains (A–D). The location of the side chains is arbitrary, since their distribution on the backbone is not known.

suggestion that the four side chains are distributed in a well-defined manner [23].

The availability of glycanases that generate fragments from RG-II would be of considerable value for determining the distribution of the oligoglycosyl side chains. However, RG-II is resistant to degradation by all the known pectic-degrading enzymes. Indeed, RG-II has been isolated, in an apparently intact form, from Pectinol AC, a commercial pectolytic enzyme preparation [21], from wine [24] and from fruit juices obtained with liquefying enzyme preparations [4]. We have recently isolated a strain of *Penicillium daleae* that grows on RG-II as the sole carbon source [25]. We now report the partial fragmentation of monomeric rhamnogalacturonan II (mRG-II) using a cell-free extract from *P. daleae*. The major oligoglycosyl fragment generated has been purified and structurally characterized. The locations of the aceric acid- and Dha-containing side chains on the RG-II backbone are discussed.

2. Experimental

Isolation and characterization of wine monomeric RG-II.—RG-II (Fraction RG-II2) was isolated from red wine as previously described [26]. This fraction was shown, by high-resolution size-exclusion chromatography (HPSEC) on a Superdex-75 HR-10/30 column, to contain 98% mRG-II. The monomer was shown, by matrix-assisted laser desorption/ionization time of flight mass spectrometry, to have a molecular mass of ~ 4.7 kDa [7,26]. Glycosyl-residue and glycosyl-linkage composition analyses confirmed that the structure of wine mRG-II was consistent with the known structural features of primary cell-wall RG-II.

Saponification and reduction of mRG-II.—Monomeric RG-II (270 mg) was de-esterified by treatment for 2 h at 4 °C with 50 mM NaOH (50 mL). The solution was neutralized with glacial AcOH and then dialyzed against deionized water. De-esterified mRG-II was then treated for 6 h at 4 °C with M NH_4OH (90 mL) containing 0.3 M $NaBH_4$ to convert the reducing galacturonic acid of the RG-II backbone to L-galactonic acid. The solution was acidified to destroy the excess $NaBH_4$, dialyzed against water and then freeze-dried. The resulting product was shown, by HPSEC, to contain 90% $NaBH_4$-reduced mRG-II (mRG-II′ol) and 10% dRG-II-B′ol. We assume that a partial dimerization of mRG-II′ol occurred during the reduction treatment.

Preparation of a cell-free extract from P. daleae *containing RG-II-degrading glycanases.*—A strain of *P. daleae*, isolated from soil for its ability to utilize RG-II as the sole carbon source [25], was grown for 15 days on a liquid salt medium (170 mL) containing mRG-II (1 g). The fragmentation of mRG-II in the growth medium was monitored by HPSEC using a Shodex OH-Pak KB-803 column, a KB-805 column and a KB-800 guard column (Showa Denko; Japan) connected in series. The columns were eluted at 1 mL/min with 0.1 M $LiNO_3$ and the eluant monitored with an RI detector (Erma ERC-7512, Japan). The mRG-II was not completely degraded even after 15 days of fungal growth. Moreover, no RG-II-degrading glycanases were detected in the fungal growth medium [25]. Thus, a crude cell-free extract was used as a source of RG-II-degrading enzymes. The mycelium (1.2 g fresh weight) was separated from the growth medium by filtration and mixed with glass beads of (0.45–0.5 mm diameter, 5 g) in 50 mM morphilino–ethane–sulfonic acid, pH 6, containing 1 mM DTT and 1 mM phenyl–methyl–sulfonyl–fluoride (6 mL). The mixture was then crushed for 5 min at 4 °C using an MM 2000 Retsch apparatus (Bioblock, France). The suspension was centrifuged (3000*g*, 5 min). The supernatant was shown, by the Lowry procedure, to contain ~ 2 mg/mL protein content.

Degradation of mRG-II′ol by the cell-free extract from P. daleae.—A solution of mRG-II′ol (270 mg) in 50 mM sodium acetate (25 mL), pH 4.8, containing 0.02% sodium azide was treated for 200 h at 25 °C with the cell-free extract (2 mL, approximately 4 mg of protein). The solution was then fractionated in 5 separate aliquots on a Superdex-30 column (1.6×60 cm) eluted at 1 mL/min with 30 mM ammonium formate, pH 5.2. Five fractions were collected (see Fig. 2(A)) and freeze-dried

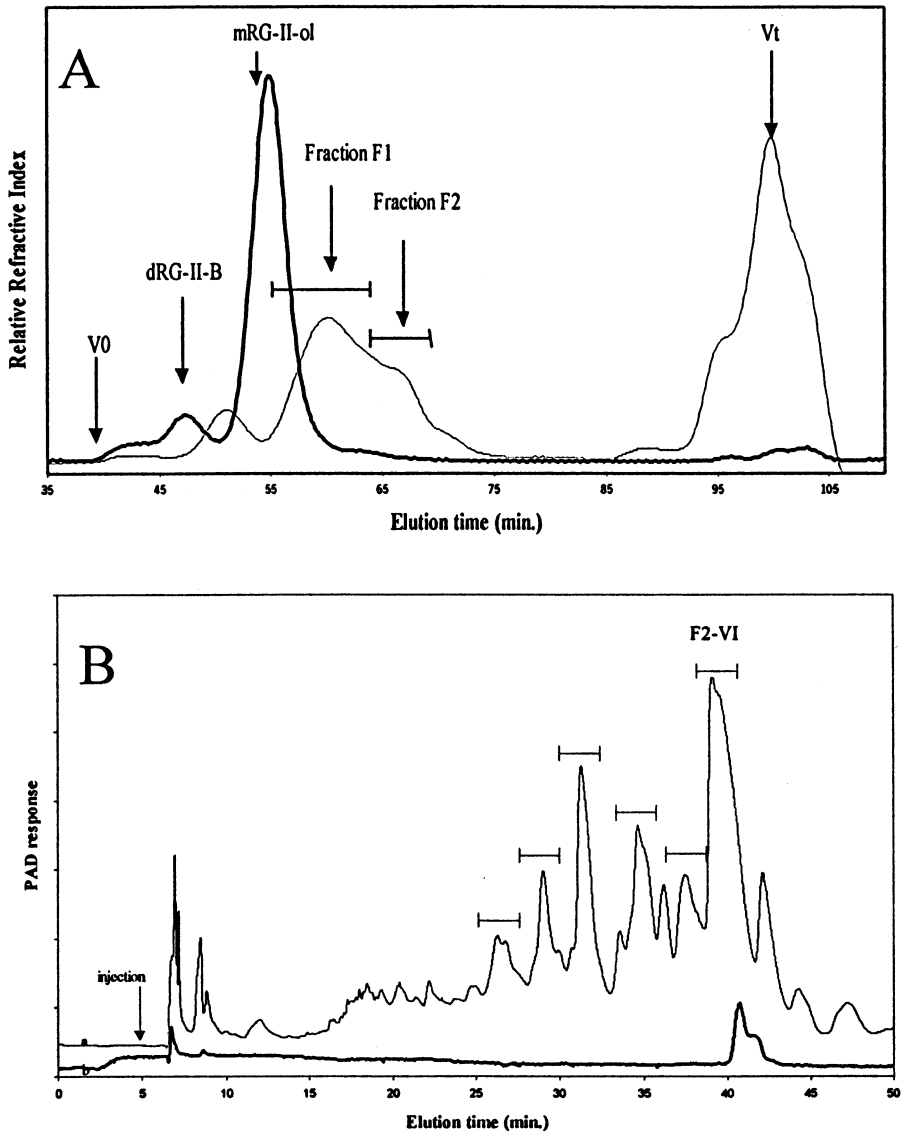

Fig. 2. Separation of the oligoglycosyl fragments generated by treating mRG-II′ol with a cell-free extract from *P. daleae*. (A) HPSEC of the products (thin line) resulting from enzymatic fragmentation of mRG-II′ol (thick line). (B) HPAEC-PAD chromatography of the oligosaccharides in Fraction 2 (see panel A). The peaks were collected as shown (thin line), neutralized and desalted. The quantitatively major peak (Fraction F2-VI, thick line) was then structurally characterized.

four times to remove the volatile ammonium formate. The fraction eluting between 63 and 68 min (Fraction F2 in Fig. 2(A)) was then fractionated by high-performance anion-exchange chromatography (HPAEC) on a Dionex BioLC (Dionex, USA) equipped with a pulsed amperometric detector, a CarboPac PA-1 column (0.4×25 cm, Dionex), and a CarboPac PA-1 guard column (0.4×5 cm). The column was eluted with 200 mM sodium acetate (0–10 min) followed by a linear gradient up to 400 mM (10–15 min) and then a linear gradient up to 650 mM (15–45 min), and finally a linear gradient up to 900 mM (45–60 min). Nine fractions were collected manually (see Fig. 2(B)) and immediately neutralized by the addition of 50% AcOH. The fractions were desalted by HPSEC using a Superdex-30 HR 10/30 column and then repeatedly freeze-dried to remove ammonium formate. The predominant fraction (~ 800 μg) isolated by HPAEC was treated for 5 min at 100 °C with aq 2% AcOH (1 mL) to remove the acid-labile Kdo residue. The solution was neutralized by the addition of NaOH (0.2 M), desalted on a Superdex-30 HR 10/30 column, and freeze-dried five times.

Glycosyl-residue and glycosyl-linkage composition analyses.—Neutral and acidic glycosyl residues were determined by GC analysis of their per-O-trimethylsilylated methyl glycosides [27]. The identity of each peak was confirmed by chemical ionization-mass spectrometry using a Hewlett–Packard 5973 mass-selective detector. Glycosyl-linkage compositions of the methylated and carboxyl-reduced oligosaccharides were determined by GC–EIMS analysis of the per-O-methylated alditol acetates [24].

Determination of the degree of polymerization of the oligogalacturonide backbones of the fragments generated from mRG-II′ol.—The oligoglycosyl-containing fractions generated by enzymic fragmentation of mRG-II′ol were treated for 16 h at 80 °C with 0.1 M TFA and the products formed analyzed by HPAEC-PAD [26,28]. The degree of polymerization of the oligogalacturonides was determined by comparison with the elution times of standard $(1\rightarrow4)$-linked α-D-oligogalacturonides generated by treating a solution of polygalacturonic acid (0.2% w/w) in 0.1 M sodium acetate, pH 4.8, for 16 h at 40 °C with a purified endo-polygalacturonase (4 nkat/mL, Megazyme, Australia).

*Generation of α-D-Gal*p*A-(1→4)-α-D-Gal*p*A-(1→3)-L-galactonate.*—A solution of trigalacturonic acid (15 mg, Sigma) in 1 M NH_4OH (2 mL) was treated for 2 h at 20 °C with $NaBH_4$ (10 mg/mL) to convert the reducing Gal*p*A to L-galactonate. The solution was acidified with glacial AcOH and then concentrated to dryness under a flow of nitrogen gas. The residual borate was removed by repeated codistillation with MeOH containing 10% (v/v) Gl HoAc and then with MeOH. A solution of the $NaBH_4$-reduced material in water (1 mL) was desalted by elution through an OnGuard H^+ column (Dionex Corp) with water and the eluate freeze dried. The $NaBH_4$-reduced trigalacturonic acid was concentrated to dryness, dissolved in ^2H_2O (1 mL, 99.6% isotopically enriched, Cambridge Isotopes), and freeze dried. The material was then dissolved in ^2H_2O (0.7 mL, 99. 96% isotopically enriched) and solid Na_2CO_3 ($\sim$1 mg) added. The solution was then adjusted to pH 6.5 by gently purging the solution with CO_2 gas.

Electrospray-ionization mass spectrometry (ESMS) analysis of the fragments.—ESMS analysis was performed with a PE-Sciex API-I Plus mass spectrometer (Sciex, Thornill, Ontario, Canada) operated in the negative-ion mode with a needle potential of -3.5 kV and an orifice potential of -60 V. Solutions of oligosaccharides (100 μg) in 1:1 MeOH–water (100 μL) were adjusted to pH 10 by the addition of 1 M NH_4OH and then infused into the electrospray source at 5 μL/min using a Harvard 22 syringe pump. Spectra were obtained between m/z 400 and 1300 with a step size of 0.1 amu and a dwell time of 25 ms. Spectra were analyzed using Sciex HyperMass/MacSpec software.

One- and two-dimensional ^1H NMR spectroscopy.—Fraction AT-F2-VI was dissolved in 99.96% isotopically enriched ^2H_2O and then freeze-dried. The residue was dissolved in 99.96% enriched ^2H_2O (100 μL) and solid anhydrous Na_2CO_3 ($\sim$1 mg) was added to make the solution alkaline. Dry CO_2 gas was bubbled through the solution for 30 s to bring the pH to $\sim$6.5. The sample was then transferred to a 5 mm ^2H_2O-matched Shegemi NMR tube. COSY [29], TOCSY [30], NOESY [31] and HSQC [32] spectra were recorded at 298 K and 600 MHz with a Varian Inova 600 NMR spectrometer. The TOCSY mixing time was 94 ms. Two NOESY spectra were recorded, with mixing times of 200 and 600 ms, respectively. COSY and HSQC were recorded using pulsed field gradients for coherence selection [33]. In a typical two-dimensional ($^1H-^1H$) spectrum, 512 transients of 1024 data points were recorded with a spectral width of 3600 Hz in both dimensions, and the data were processed with zero filling to obtain a 2048×2048 matrix. Chemical shifts were measured relative to internal acetone at δ 2.225.

3. Results

Production of a cell-free extract of P. daleae *that contains mRG-II degrading glycanases.*—*P. daleae* was grown on mRG-II as the sole carbon source [25] and the extent of fragmentation of mRG-II monitored by HPSEC anal-

ysis. The production of fungal biomass was correlated to the degradation of mRG-II. No RG-II-fragmenting enzymes were present in the growth medium [25]. However, a cell-free extract prepared from the fungal mycelium did contain mRG-II-fragmenting activity.

Incubation of mRG-II-ol with P. daleae *enzymes and fractionation of the resulting fragments.*—MRG-II′ol was partially fragmented by treatment for 200 h with the cell-free extract from *P. daleae*. The fragmented material was shown, by HPSEC (see Fig. 2(A)), to contain a broad main peak (Fraction F1) with a shoulder (Fraction F2). Fraction F2 accounted for $\sim 25\%$ of the mRG-II′ol-derived molecules recovered. Glycosyl-residue composition analyses indicated that Fraction F1 contained portions of the four oligosaccharide side-chains. In contrast, Fraction F2 was enriched in those glycosyl residue that are diagnostic of side chains B, C, and D but contained only trace amounts of the three sugar residues (2-*O*-Me-Xyl, GlcA, and Fuc) that are diagnostic of side-chain A (Table 1).

Fraction F2 was fractionated by HPAEC and nine fractions (F2-I to F2-IX) collected (Fig. 2(B)). These fractions have similar but not identical glycosyl-residue and glycosyl-linkage compositions (data not shown), suggesting that they contain structurally related fragments of mRG-II. The results of ESMS analysis provided additional evidence that the nine fractions were enriched in side chains B, C and D, and that they all contained a oligogalacturonide backbone, although the length of the backbone varied between DP 4 and 7. Fraction F2-VI, the quantitatively major fraction, was selected for further structural characterization.

Table 1
Glycosyl-residue composition and degree of polymerization of the homogalacturonan backbone of the degraded fragment after purification steps in comparison with native mRG-II

Glycosyl residue [a]	mRG-II2-ol	F2	AT-F2-VI [c]
Api	8	12	14
Ara	10	4	8
Rha	13	4	8
Fuc	3	1	0
2-*O*-Me-Xyl	4	0	0
2-*O*-Me-Fuc	3	2	1
Aceric acid	2	3	7
Gal	7	11	7
GalA	34	44	40
GlcA	6	0	0
Galactonic acid	4	7	8
Dha	4	5	7
Kdo	3	7	0
dp [b]	**8–9**	**6**	**6**

[a] Mol% determined by GC analysis of the per-O-trimethylsilylated methyl glycosides.

[b] Degree of polymerization of the homogalacturonan backbone determined by HPAEC analysis.

[c] AT-F2-VI: Fraction F2-VI after acid hydrolysis treatment.

The ESMS spectrum of Fraction F2-VI contained four series of distinct peaks corresponding to the three-fold and four-fold charged $[M-3H]^{3-}/3$, $[M-4H]^{4-}/4$ and $[M-3H+n\mathrm{Na}]^{3-}/3$, $[M-4H+n\mathrm{Na}]^{4-}/4$ ions. The masses of the three-fold and four-fold charged ions were converted to their corresponding molecular-weight species (Fig. 3). The mass at 2232 corresponds to an oligosaccharide composed of five galactosyluronic acid residues, one arabinosyl, one galactosyl, one aceryl acid, one rhamnosyl, one apiosyl, one Dha, one Kdo residue and galactonic acid. The masses at 2254, 2276, 2298, 2322 and 2343 are most likely to be the corresponding natriated ($[M+n\mathrm{Na}]$) species. The presence of a structurally related oligosaccharide that does not contain a Kdo residue is suggested by the mass series beginning at 2012 amu, since the masses of these ions are each 220 amu lower than the series of masses beginning at 2232. The presence of two fragments in Fraction F2-VI that differed only by the presence of a single Kdo residue was confirmed by ^{1}H NMR spectroscopy and by glycosyl-residue composition analysis (data not shown). The assignment of the ^{1}H NMR spectrum of Fraction F2-VI was complicated by the presence of Kdo in non-stoichiometric amounts. Thus, Fraction F2-VI was treated with hot aqueous 2% AcOH to selectively remove the Kdo residue [19] and thereby generate Fraction AT-F2-VI.

Glycosyl-residue composition analysis of AT-F2-VI (Table 1) confirmed that Kdo had been removed. The presence of galactonic acid showed that enzymatic fragmentation had occurred at the non-reducing terminal end of

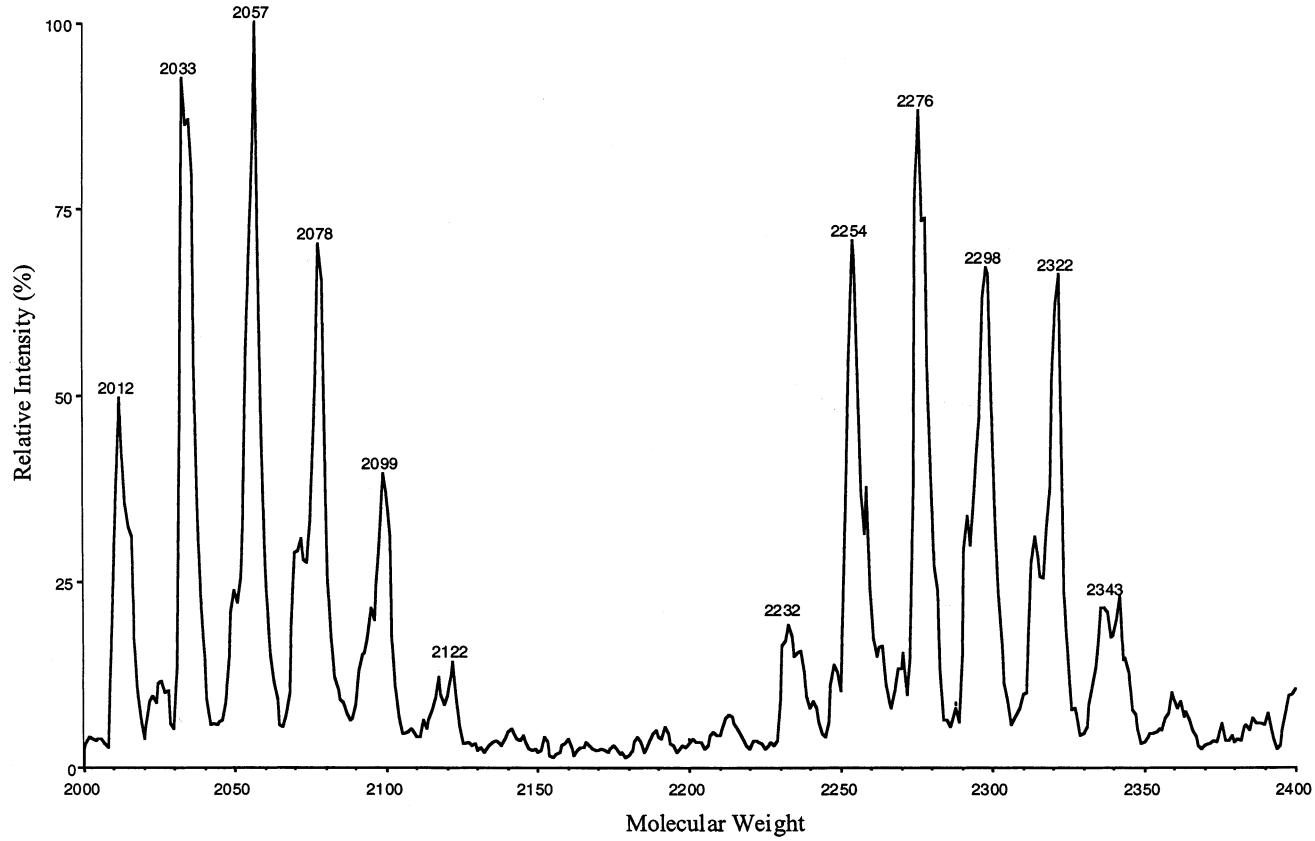

Fig. 3. The reconstructed negative-ion ES mass spectrum of Fraction F2-VI. The negative-ion mass spectrum of F2-VI contained ions corresponding to $[M-2H]^{2-}/2$ and $[M-2H+n\mathrm{Na}]^{2-}/2$. These ions were converted to their corresponding singly charged species.

mRG-II-ol. Backbone fragments were generated by treating Fraction AT-F2-VI for 1 h at 80 °C with 0.1 M TFA. The hydrolyzate was analyzed by HPAEC-PAD and shown to contain a series of components that cochromatographed with standard (1→4)-linked α-D-oligogalacturonides. The largest component had a DP of 6, thereby indicating that the oligosaccharide in Fraction AT-F2-VI had a backbone composed of five galactosyluronic acid residues and galactonic acid. These results when taken together with the results of ESMS analysis of Fraction F2-VI suggest that the quantitatively major oligosaccharide in Fraction AT-F2-VI is composed of five galactosyluronic acid residues, one arabinosyl, one galactosyl, one aceryl acid, one rhamnosyl, one apiosyl, one Dha residue and galactonic acid.

Characterization of the oligoglycosyl fragment in Fraction AT-F2-VI by 1 and 2D ^1H NMR spectroscopy.—The primary structure of the major component of Fraction AT-F2-VI was established by 1D and 2D NMR spectroscopy in ^2H_2O, pH ~6.5 (Figs. 4–7). Two groups of resonances, which were distin-

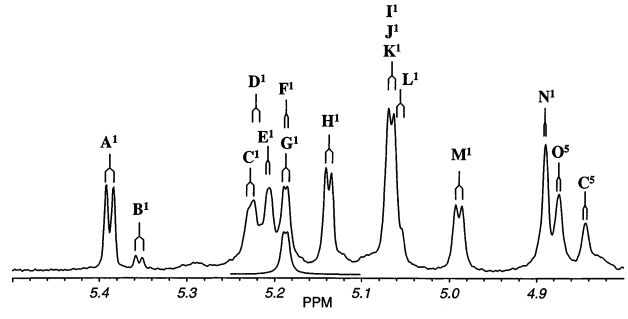

Fig. 4. A portion of the anomeric proton region of the one-dimensional ^1H NMR spectrum of the oligosaccharides in Fraction AT-F2-VI. Isolated spin systems are named by uppercase letters. Superscript numbers refer to the atomic numbering system for the spin system. For example, **A**^{1} designates H-1 of spin system **A**. Due to overlap of the H-1 resonances of spins system **F** and **G**, the scalar coupling constant $^3J_{1,2}$ for **G** could not be measured directly from the 1D ^1H NMR spectrum. Therefore, the anomeric proton resonances of **F** and **G** were simulated and added together in a 1:5 ratio to reproduce the observed multiplet shape, as shown beneath the actual spectrum.

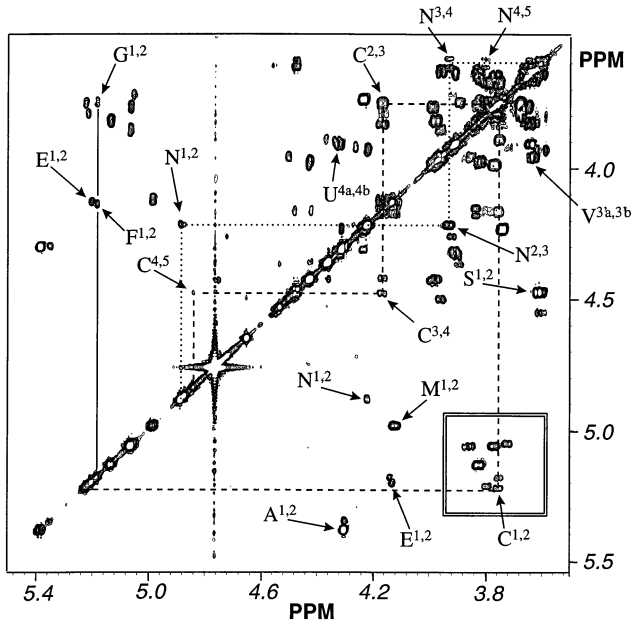

Fig. 5. COSY spectrum of Fraction AT-F2-VI. Uppercase letters in the cross-peak labels indicate specific spin systems, and superscript numbers indicate the atomic numbering system for the spin system. For example, $\mathbf{A}^{1,2}$ indicates the H-1-H-2 cross-peak for spin system **A**. The solid, vertical line illustrates the chemical shift degeneracy of the H-1 resonances of spin systems **F** and **G** (see Fig. 4). The [H-1, H-2] cross-peaks of the eight different α-D-GalA*p* spin systems observed in the spectrum are surrounded by a double-lined box. (Note that the [H-1, H-2] cross-peaks of the **J** and **K** systems overlap.) The scalar connectivity for spin systems **C** (dashed lines) and **N** (dotted lines) is also indicated.

guished by differences in their signal intensities, were observed in these spectra (Fig. 4, Tables 2 and 3), indicating that AT-F2-VI contained two oligosaccharides in a ratio of approximately 6:1. The resonances of 22 isolated spin systems, each indicated by an uppercase letter (see Table 2), were assigned. Fifteen of these spin systems were assigned to the major component and seven were assigned to the minor component. The structure of the major component was determined by analyses of the scalar and dipolar interactions of the protons comprising the 15 spin systems.

The structure of the oligogalacturonide backbone of AT-F2-VI. The resonances of eight unique α-D-Gal*p*A spin systems were observed in the ^{1}H NMR spectra of AT-F2-VI (Figs. 4 and 5, Table 2). The resonance intensities of five of these spin systems (**C**, **G**, **H**, **I** and **J**) show that they correspond to α-D-Gal*p*A residues in the major oligosaccharide component. These five spin systems were completely assigned by tracing scalar connectivities in 2D COSY and TOSCY spectra (Table 2). The ^{1}H–^{1}H scalar connectivities of these α-D-Gal*p*A spin systems can be traced from H-1 to

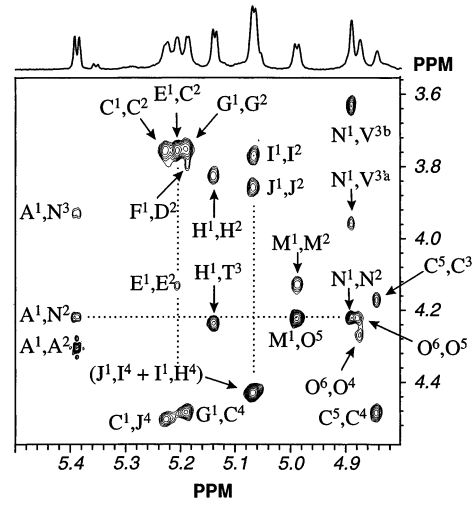

Fig. 6. Portion of the NOESY spectrum (with 200 ms mixing time) of Fraction AT-F2-VI containing most of the interglycosidic crosspeaks (see Fig. 4 for nomenclature). The components of the cross-peak labeled $(\mathbf{J}^1, \mathbf{I}^4) + (\mathbf{I}^1, \mathbf{H}^4)$ were assigned as such because the alternative $(\mathbf{J}^1, \mathbf{H}^4) + (\mathbf{I}^1, \mathbf{I}^4)$ does not make sense in light of the large H-1–H-4 distance in an α-D-GalA*p* residue and the observation of diagnostic cross-peaks in other regions of the NOESY spectrum (see text). Other overlapping resonances could be confidently distinguished by small but significant chemical shift differences (e.g., $\mathbf{C}^2$ vs. $\mathbf{G}^2$ and $\mathbf{N}^2$ vs. $\mathbf{O}^5$). Intraglycosidic cross-peaks that establish the connectivity of $\mathbf{O}^6$ and $\mathbf{C}^5$ to their respective spin systems are also indicated.

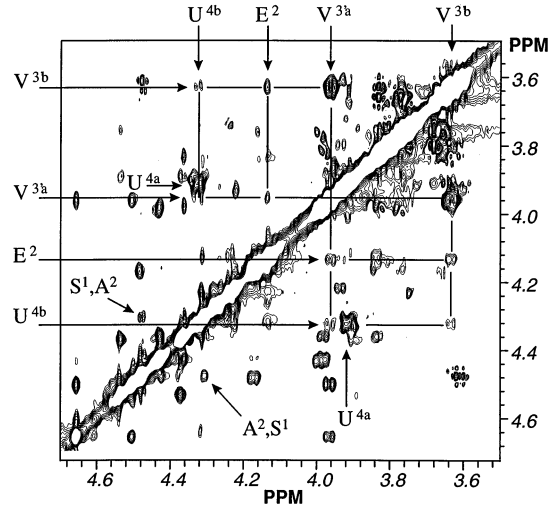

Fig. 7. Portion of the NOESY spectrum (with 200 ms mixing time) of Fraction AT-F2-VI containing cross-peaks that establish the spin systems **E**, **U**, and **V** as part of the same β-D-apiosyl residue (see Fig. 9). The $\mathbf{S}^1$, $\mathbf{A}^2$ cross-peaks, due to the (1→2) linkage of the β-D-Gal*p* residue to the α-L-AceA*f* residue, are also indicated.

Table 2
Spin systems corresponding to commonly found glycosyl residues in AT-F2-VI

Spin system	Glycosyl residue	δ H-1 ($^3J_{1,2}$) [δ C-1]	δ H-2 ($^3J_{2,3}$) [δ C-2]	δ H-3 ($^3J_{3,4}$) [δ C-3]	δ H-4 ($^3J_{4,5a}$) ($^3J_{4,5b}$) [δ C-4]	δ H-5$_{(a)}$ ($^3J_{5a,6}$) [δ C-5]	δ H-5$_b$ ($^2J_{5a,5b}$)	δ H-6$_{(a)}$ [δ C-6]	δ H-6$_b$ ($^2J_{6a,6b}$)
C	α-D-Gal*p*A	5.229 (3.9)	3.759 (10)	4.170 (<4)	4.488 (<2)	4.845	–	–	–
D* [a]	α-D-Gal*p*A (minor)	5.222 (3.9)	3.797 (10)	4.168 (<4)	4.427 (<2)	n.a. [b]	–	–	–
G	α-D-Gal*p*A	5.190 (3.5) [c]	3.754 (10)	3.896 (<4)	4.375 (<2)	4.538	–	–	–
H	α-D-Gal*p*A	5.138 (3.9) [100.1]	3.828 (10)	3.982 (<4)	4.428 (<2)	4.363	–	–	–
I	α-D-Gal*p*A	5.069 (3.9) [100.7]	3.771 (10)	3.995 (<4)	4.433 (<2)	4.758	–	–	–
J	α-D-Gal*p*A	5.069 (3.9) [100.7]	3.856 (10)	3.964 (<4)	4.505 (<2)	4.658	–	–	–
K*	α-D-Gal*p*A (minor)	5.069 (4)	3.872 (10)	3.964	4.507	n.a. [b]	–	–	–
L*	α-D-Gal*p*A (minor)	5.060 (4)	3.726 (10)	3.921 (<4)	4.266	4.724	–	–	–
M	β-L-Ara*f*	4.991 (4.8) [104.9]	4.127 (9.8) [c]	4.177 (3.4) [c]	3.840 (1.6) [c] (2.5) [c] [82.6]	3.771 [61.4]	3.662 (12.9) [c]	–	–
N	β-L-Rha*p*	4.890 (<2) [101.5]	4.223 (<5) [68.6]	3.937 (10)	3.606 (10)	3.806 (6.0)	–	1.333 [18.5]	–
R*	β-D-Gal*p* (minor)	4.558 (7.9)	3.605 (10)	3.646 (<4)	3.919 (<2)	n.a. [b]	–	n.a. [b]	n.a. [b]
S	β-D-Gal*p*	4.480 (7.9) [105.9]	3.610 (10) [72.0]	3.646 (<4) [74.1]	3.911 (<2) [70.0]	n.a. [b]	–	3.77 [62.5]	3.77
T	l-Galactonate	–	4.317 (<3)	4.239 (8)	3.745 (<3)	3.835 [d]	–	3.65 [64.7]	3.65

[a] An asterisk indicates that the spin system corresponds to a residue in the minor oligosaccharide component in the mixture.

[b] n.a. not assigned.

[c] The coupling constants $^1J_{1,2}$ for α-D-Gal*p*A **G** and several of the coupling constants for the β-L-Ara*f* **M** were estimated by spectral simulation.

[d] Tentative assignment of H-5 of galactonate **T** was made by analogy to borohydride-reduced tri-GalA (Table 5) and the observation of an interglycosidic NOE (Table 5).

Table 3
Spin systems corresponding to unusual sugar residues of AT-F2-VI

Spin system	Glycosyl residue	Resonance	Chemical shift	Scalar coupling
A	α-L-Ace*f*A	H-1	5.389	$^3J_{1,2}$ 5.0
	(see **P**)	H-2	4.306	
		C-1	99.7	
		C-2	89.9	
B* [a]	α-L-Ace*f*A	H-1	5.356	$^3J_{1,2}$ 4.8
	(minor)	H-2	4.303	
E	β-D-Api*f*	H-1	5.210	$^3J_{1,2}$ 2.2
	(see **U**, **V**)	H-2	4.135	
		C-1	111.3	
F*	β-D-Api*f*	H-1	5.190	$^3J_{1,2}$ 1.8 [b]
	(minor)	H-2	4.143	
		C-1	111.3	
O	Dha*p*A	H-3_{ax}	1.848 [b]	$^2J_{3ax,3eq}$ 12.5 [c]
				$^3J_{3ax,4}$ 10
		H-3_{eq}	2.249 [b]	$^3J_{3eq,4}$ 4.0
		H-4	4.277	$^3J_{4,5}$ 3.5
		H-5	4.227	$^3J_{5,6}<2$
		H-6	4.877	
P	α-L-Ace*f*A	H-4	4.786	$^3J_{5,6}$ 6.6
	(See **A**)	H-5, H-5′, H-5″	1.172	
		C-5	14.4	
Q*	α-L-Ace*f*A	H-4	4.526	$^3J_{5,6}$ 6.5
	(minor, see **B***)	H-5, H-5′, H-5″	1.208	
U	β-D-Api*f*	H-4_b	4.325	$^2J_{4a,4b}$ 11
	(see **E**, **V**)	H-4_a	3.912	
		C-4	76.1	
V	β-D-Api*f*	H-$3'_a$	3.963	$^2J_{3'a,3'b}$ 11
	(see **E**, **U**)	H-$3'_b$	3.632	
		C-3′	71.9	

[a] An asterisk indicates that the spin system corresponds to a residue in the minor oligosaccharide component in the mixture.
[b] The coupling constant $^1J_{1,2}$ for β-D-Api*f* **F** was estimated by spectral simulation.
[c] Dha*p*A H-3_{ax} and H-3_{eq} multiplets were both broadened due to microheterogeneity. Listed scalar coupling constants were estimated by spectral simulation.

H-5. This is in direct contrast to Gal*p* spin systems, where the very small value of $^3J_{4,5}$ typically precludes the observation of a scalar connectivity between H-4 and H-5. Many of the α-D-Gal*p*A resonance assignments for AT-F2-VI were confirmed by the observation of intraglycosidic NOESY cross-peaks (Table 4) that arise due to the spatial proximity of H-3, H-4, and H-5 within each of these residues.

The sequence and linkage of the α-D-Gal*p*A residues in the backbone of the predominant oligosaccharide was determined by analysis of the NOESY spectrum. Strong NOESY cross-peaks were observed between H-1 of each α-D-Gal*p*A residue and H-4 of the adjacent residue (Fig. 6, Table 4), consistent with the previously demonstrated α-(1→4) linkage of the D-Gal*p*A residues in the RG-II backbone [22]. Assignment of the glycosyl sequence is complicated by resonance overlap, as H-1 of **I** and **J** have the same chemical shift (δ 5.069), and H-4 of **H** and **I** have similar chemical shifts (δ 4.428 and δ 4.433). Two different backbone sequences are consistent with the pattern of interglycosidic H-1/H-4 NOE contacts. The first, **G**→**C**→**J**→**I**→**H**, contains

all five α-D-Gal*p*A residues, including residue **I**, which is placed between residues **J** and **H**. The second, **G**→**C**→**J**→**H**, does not contain residue **I**, and residue **J** is linked directly to **H**. However, other interglycosidic NOESY cross-peaks indicate that the sequence with all five residues is correct. Specifically, a weak cross-peak between H-5 of **J** and H-2 of **I** indicates that residues **J** is glycosidically linked to **I** and that the two residues fold together in an accordion-like fashion, as previously proposed for adjacent residues in a homogalacturonan chain [34]. The **G**→**C** glycosidic linkage is confirmed by a cross-peak between H-5 of **G** and H-2 of **C**. Together, these results indicate that the sequence of α-D-Gal*p*A residues in the backbone of the major oligosaccharide is **G**→**C**→**J**→**I**→**H** (see Fig. 8).

The (1→4)-linked α-D-Gal*p*A at the reducing end of the molecule was converted to (1→3)-linked L-galactonic acid by treatment with $NaBH_4$ prior to enzymic fragmentation of RG-II; the nomenclature describing Gal*p*A and galactonic acid is dependent on their oxidation states. The L-galactonic acid residue was most likely converted to L-galactonolactone under the acidic conditions used to remove borate from the chemical reaction. However, prior to NMR analysis, Fraction AT-F2-VI was exposed to 100 mM NaOH, which likely hydrolyzes the galactonolactone ring and thereby regenerates galactonic acid. The ^1H NMR spectra of α-D-Gal*p*A-(1→4)-α-D-Gal*p*A-(1→3)-L-galactonic acid in ^2H_2O, pH ~6.5, were used to determine chemical shifts and coupling constants that characterize the γ-lactone and open-chain forms of galactonic acid substituted at O-3 with α-D-Gal*p*A (Table 5). These data were then used to establish the chemical form of the galactonic acid residue in Fraction AT-F2-VI. Three resonances of spin system **T** were assigned to H-2, H-3, and H-4 of 3-linked L-galactonate (open-chain form) by the close correspondence of their chemical shifts and coupling constants (Table 2) to those of the $NaBH_4$-reduced trigalacturonic acid. No resonances corresponding to the γ-galactonolactone were observed in the ^1H NMR spectra of AT-F2-VI. Due to resonance overlap, it was

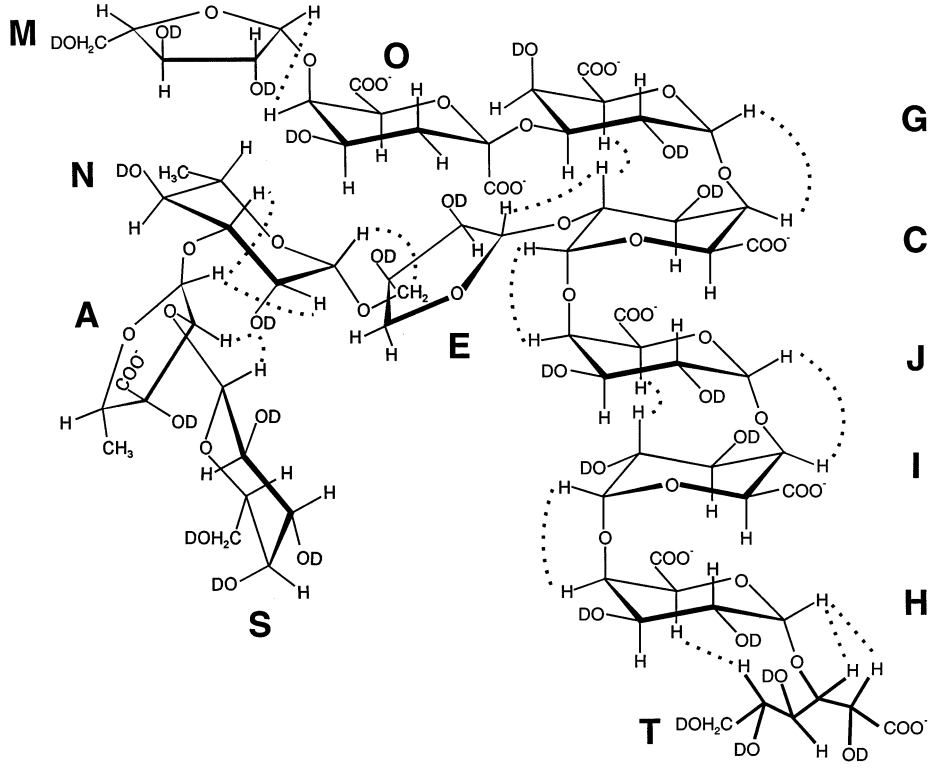

Fig. 8. The deduced glycosyl sequence of Fraction AT-F2-VI. The deduced glycosyl sequence of Fraction AT-F2-VI is shown together with the diagnostic inter-glycosidic NOE contacts (·····). The proposed location of the α-L-Ara*f*-(1→5)-β-D-Dha*p*A side chain is based solely on the results of glycosyl-linkage compostion analysis.

Table 4
Assignment of cross-peaks [a] in the NOESY spectrum of AT-F2-VI

δ (ppm) [b]	Residue (spin system) proton	δ (ppm) [b]	Residue (spin system) proton	Comments
5.389	AceA (**A**) H-1	4.306	AceA (**A**) H-2	COSY artifact in this crosspeak
		4.224	Rha (**N**) H-2	NOEs to H-2 and
		3.937	Rha (**N**) H-3	H-3 have similar intensity
5.229	GalA (**C**) H-1	4.505	GalA (**J**) H-4	**C** → **J** by (1 → 4) linkage
		3.759	GalA (**C**) H-2	intraglycosidic
		4.325	Api (**E**) H-4b	(very weak) interaction of GalA (**C**) and Api (**E**)?
		4.658	GalA (**J**) H-5	(weak) confirms **C** → **J** linkage
5.222	GalA (**D***) H-1	3.797	GalA (**D*** [c]) H-2	(weak)
5.210	Api (**E**) H-1	4.135	Api (**E**) H-2	intraglycosidic
		3.759	GalA (**C**) H-2	**E** → **C** by (1 → 2) linkage
5.190	GalA (**G**) H-1	4.485	GalA (**C**) H-4	**G** → **C** by (1 → 4) linkage
		3.755	GalA (**G**) H-2	intraglycosidic
5.190	Api (**F***) H-1	3.798	GalA (**D***) H-2	**F*** → **D*** by (1 → 2) linkage
5.139	GalA (**H**) H-1	4.318	Galactonate (**T**) H-2	(weak) **H** → **T** by (1 → 3) linkage
		4.239	Galactonate (**T**) H-3	(strong) **H** → **T** by (1 → 3) linkage
		3.828	GalA (**H**) H-2	intraglycosidic
5.068	GalA (**I**) H-1 GalA (**J**) H-1	4.432	GalA (**H**) H-4	(broad, very strong)
			GalA (**I**) H-4	**J** → **I** → **H** by (1 → 4) linkages (see text)
		4.366	GalA (**H**) H-5	(weak) confirms linkage → **H**
		3.858	GalA (**J**) H-2	intraglycosidic
		3.773	GalA (**I**) H-2	intraglycosidic
5.061	GalA (**I**) H-1	3.727	GalA (**I**) H-2	intraglycosidic
4.992	Ara (**M**) H-1	4.227	DHA (**O**) H-5	**M** → **O** by (1 → 5) linkage
		4.128	Ara (**M**) H-2	intraglycosidic
4.890	Rha (**N**) H-1	4.224	Rha (**N**) H-2	intraglycosidic
		3.964	Api (**V**) H-3′a	**N** → **V** by (1 → 3′) linkage
		3.633	Api (**V**) H-3′b	**E**/**U**/**V** constitute Apiose
4.876	DHA (**O**) H-6	4.276	DHA (**O**) H-4	correlates DHA H6 to
		4.227	DHA (**O**) H-5	the rest of the residue
4.845	GalA (**C**) H-5	4.488	GalA (**C**) H-4	confirms **C** spin system
		4.172	GalA (**C**) H-3	
4.756	GalA (**I**) H-5	4.435	GalA (**I**) H-4	confirms **I** spin system
		3.995	GalA (**I**) H-3	
4.725	GalA (**L***) H-5	4.266	GalA (**L***) H-4	confirms **L*** spin system
4.658	GalA (**J**) H-5	4.505	GalA (**J**) H-4	confirms **J** spin system
		3.964	GalA (**J**) H-3	
		3.772	GalA (**I**) H-2	(weak) suggests folding together of **I** and **J**
4.538	GalA (**G**) H-5	4.374	GalA (**G**) H-4	confirms **G** spin system
		3.896	GalA (**G**) H-3	(H3/H5 NOE is weak)
		3.759	GalA (**C**) H-2	(weak) suggests folding together of **C** and **G**
4.505	GalA (**J**) H-4	3.965	GalA (**J**) H-3	intraglycosidic
4.486	GalA (**C**) H-4	4.171	GalA (**C**) H-3	intraglycosidic
4.480	Gal (**S**) H-1	4.306	AceA (**A**) H-2	**S** → **A** by β linkage β-Gal*p*-(1 → 2)-AceA*f*

Table 4 (Continued)

δ (ppm) [b]	Residue (spin system) proton	δ (ppm) [b]	Residue (spin system) proton	Comments
4.432	GalA (**I**) H-4	3.995	GalA (**I**) H-3	intraglycosidic
4.427	GalA (**H**) H-4	4.364	GalA (**H**) H-5	confirms **H** spin system
		3.981	GalA (**H**) H-3	
4.427	GalA (**D***) H-4	4.169	GalA (**D***) H-3	weak, intraglycosidic
4.373	GalA (**G**) H-4	3.899	GalA (**G**) H-3	intraglycosidic
4.364	GalA (**H**) H-5	4.239	Galactonate (**T**) H-3	(weak) suggests folding of **T** onto **H**
		3.984	GalA (**H**) H-3	intraglycosidic
		3.835	Galactonate (**T**) H-5	tentative assignment by analogy to galactonate H5 of reduced tri-GalA
4.325	Api (**U**) H-4b	3.964	Api (**V**) H-3′a	correlate spin systems
		3.914	Api (**U**) H-4a	**U** and **V** as constituents of the apiosyl residue
		3.633	Api (**V**) H-3′b	
4.307	AceA (**A**) H-2	1.172	AceA (**P**) H-5	in NOESY with 600 ms mixing time (very weak); confirms AceA residue
4.239	Galactonate (**T**) H-3	3.747	Galactonate (**T**) H-4	COSY artifact in this crosspeak
4.224	Rha (**N**) H-2	4.937	Rha (**N**) H-3	intraglycosidic
4.136	Api (**E**) H-2	3.964	Api (**V**) H-3′a	correlate spin systems
		3.633	Api (**V**) H-3′b	**E** and **V** as constituents of the apiosyl residue
3.964	Api (**V**) H-3′a	3.633	Api (**V**) H-3′b	

[a] All cross-peaks are listed with the downfield resonance in column 1 and the upfield resonance in column 3. Except where noted, all data is taken from the NOESY spectrum recorded with a mixing time of 200 ms.

[b] Chemical shifts reported here were measured directly from the NOESY spectrum. These values are within 0.002 ppm of the shifts listed in Tables 2 and 3.

[c] An asterisk indicates that the spin system corresponds to a residue in the minor oligosaccharide component in the mixture.

not possible to trace $^1H-^1H$ scalar connectivities through to H-5, H-6a, and H-6b of the L-galactonate residue. These three resonances were tentatively assigned on the basis of cross-peaks in the NOESY and HSQC spectra (Table 2).

Table 5
Spin systems of the two forms of sodium borohydride-reduced tri-GalA

Form	Glycosyl residue	δ H-1 ($^3J_{1,2}$)	δ H-2 ($^3J_{2,3}$)	δ H-3 ($^3J_{3,4}$)	δ H-4 ($^3J_{4,5}$)	δ H-5 ($^3J_{5,6a}$) ($^3J_{5,6b}$)	δ H-6_a	δ H-6_b ($^2J_{6a,6b}$)
Open chain	terminal α-D-Gal*p*A	5.055 (4.0)	3.720 (10.3)	3.905 (3.5)	4.257 (<2)	4.742		
	internal α-D-Gal*p*A	5.136 (4.0)	3.818 (10.5)	3.984 (3.4)	4.420 (<2)	4.365		
	L-galactonate		4.317 (1.9)	4.239 (7.8)	3.741 (2)	3.832 (~7) [a] (~7) [a]	3.65 [a]	3.65 [a]
Lactone	terminal α-D-Gal*p*A	5.074 (4.0)	3.738 (10.4)	3.915 (3.5)	4.269 (<2)	4.845		
	internal α-D-Gal*p*A	5.328 (3.8)	3.918 (10.5)	4.015 (3.4)	4.437 (<2)	4.276		
	L-galactono-γ-lactone		4.838 (8.1)	4.582 (7.9)	4.511 (1.9)	3.906 (~7) [a] (~7) [a]	3.67 [a]	3.67 [a]

[a] H-6_a is nearly degenerate with H-6_b for both L-galactonate and L-galactono-γ-lactone, resulting in strong coupling. Only the apparent (first-order) scalar coupling constants are listed here.

A strong NOESY crosspeak correlating H-1 of **H** and H-3 of **T** (Fig. 6 and Table 4) indicates that α-D-Gal*p*A residue **H** is linked to O-3 of the L-galactonate residue. This linkage is confirmed by two weak cross-peaks in the NOESY spectrum (H-1 of **H** to H-2 of **T**, and H-5 of **H** to H-3 of **T**). An additional cross-peak of moderate intensity was observed between H-5 of **H** and a resonance tentatively assigned as H-5 of **T**. The H-5 of 3-linked L-galactonate (**T**) corresponds to H-2 of the 4-linked D-Gal*p*A residue from which it was derived. Thus, the NOESY cross-peak correlating H-5 of **T** to H-5 of **H** is analogous to the interglycosidic H-5/H-2 cross-peaks resulting from the **G**→**C** and **J**→**I** glycosidic linkages. Taken together these results allow the sequence of backbone acidic residues of the predominant oligosaccharide in AT-F2-VI to be extended to include the L-galactonate residue, i.e., **G**→**C**→**J**→**I**→**H**→**T** (see Fig. 8).

The structure and location of the apiosyl-containing side chain of AT-F2-VI.—Two branched chain sugars, one of which is apiose, are present in Fraction AT-F2-VI. The branched structure of apiose results in protons in three isolated spin systems (H-1/H-2; H-3′a/H-3′b; and H-4a/H-4b in Fig. 9). Spin systems **E**, **U**, and **V** are each composed of two scalar-coupled protons, and were assigned to the apiosyl residue in the major oligosaccharide component of AT-F2-VI. The chemical shifts (δ 5.210 and 4.135) and scalar coupling constant ($^3J_{1,2} = 2.2$ Hz) of the two protons of spin system **E** indicate that they are H-1 and H-2 of a furanosyl residue. Spin systems **U** and **V** each have NMR parameters (Table 3) consistent with their assignment as geminal pairs of protons. The two protons (H-3′$_a$ and H-3′$_b$) of **V** are both in NOE contact with H-2 of **E** and H-4$_b$ of **U** (Fig. 9 and Table 4). Neither H-1 of **E** nor H-4$_a$ of **U** are in NOE contact with either of the protons of **V**. This combination of NOE contacts (see Fig. 9) is fully consistent with the assignment of **E**, **U**, and **V** to the apiosyl residue if it is assumed that the C-3–C-3′ bond is free to rotate through 90° or more. Based on the small value (2.2 Hz) of $^3J_{1,2}$, protons, H-1 and H-2 of **E** were assigned as having the trans configuration [35,36], which in this case corresponds to the β anomer. Furthermore, the chemical shift of C-1 of **E** is unusually high (δ 111.3). These results, along with additional parameters (see Tables 3 and 4), are strong evidence that **E**, **U** and **V** constitute a β-D-Api*f* residue [36]. Spin system **F**, which is homologous to **E**, was assigned as H-1 and H-2 of a β-D-apiosyl residue in the minor oligosaccharide component of AT-F2-VI.

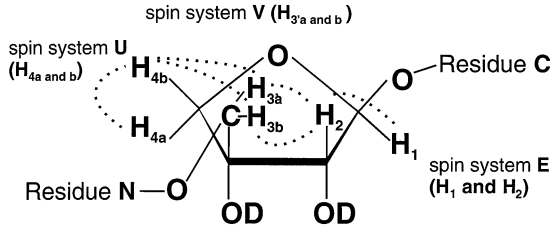

Fig. 9. The β-D-apiofuranosyl residue in Fraction AT-F2-VI with intraglycosidic NOE contacts (·····) between spin systems **E**, **U**, and **V**.

A strong interglycosidic cross-peak (Fig. 6 and Table 4) correlating H-1 of **E** (the anomeric proton of the β-D-apiosyl residue) and H-2 of **C** in the NOESY spectrum of AT-F2-VI indicates that the apiosyl residue is glycosidically linked to O-2 of α-D-Gal*p*A residue **C** (see Fig. 8). Such a result is consistent with previous analyses demonstrating that apiosyl residues are attached to the homogalacturonan backbone of RG-II via a (1→2) linkage [20,22].

Spin system **N** is assigned as an L-Rha*p* residue. The anomeric proton (H-1) and the methyl protons (H-6) of **N** are both resolved. Thus, the connectivity of the entire residue in the COSY and TOCSY spectra can be traced (see Fig. 6). Two cross-peaks in the NOESY spectrum of AT-F2-VI (Fig. 6 and Table 4) show that H-1 of **N** comes in close proximity to both resonances (H-3′$_a$ and H-3′$_b$) of spin system **V**, (i.e., C-3′ of the β-D-apiosyl residue), and thereby indicate that L-Rha*p* residue **N** is glycosidically linked to the apiosyl residue via a (1→3′) linkage (see Fig. 8). This is consistent with the previously published structure of RG-II [17]. The scalar coupling constant $^3J_{1,2}$ of a rhamnopyranosyl residue does not provide any information regarding its anomeric configuration. Nevertheless, the chemical shift of H-1 of **N** (δ 4.890) is consistent with the β-configuration, as previously proposed for the rhamnosyl residue linked to O-3′ of apiose in RG-II [17]. Rigor-

ous determination of the anomeric configuration of rhamnosyl residue **N** would require an accurate measurement of the one-bond heteronuclear coupling constant ($^1J_{C1,H1}$) [37]. This was not possible due the small amount of Fraction AT-F2-VI that was available.

The oligosaccharides in Fraction AT-F2-VI contain aceric acid, a branched chain sugar that contains two isolated spin systems (Fig. 8). One of these spin systems, consisting of a methyl group (H-5, H-5′, and H-5″) and a methine proton (H-4), is readily identified in the COSY and TOCSY spectra. Two such 4-spin systems (**P** and **Q**) were observed. The resonances of spin system **P** are much more intense than those of **Q**. Thus, **P** was assigned to the aceric acid residue of the major oligosaccharide component of AT-F2-VI. Spin system **A** is composed of two resonances, identified as H-1 and H-2 of a furanosyl residue on the basis of their chemical shifts (δ 5.389 and 4.306) and scalar coupling constant ($^3J_{1,2} = 5.0$ Hz). Spin system **B** is homologous to **A**, but the resonances of **B** are much less intense, indicating that **B** is a constituent of the minor oligosaccharide component. Spin systems **A** and **B** were assigned as H-1 and H-2 of aceric acid residues since the other 2-spin (H-1/H-2) systems of AT-F2-VI had been assigned to apiosyl residues. A weak cross-peak correlating H-2 of **A** with the methyl protons of **P** was observed in the NOESY spectrum recorded with a 600 ms mixing time (see Table 4), indicating that these two spin systems are likely to be constituents of the same aceric acid residue. Such a weak NOE would be expected for this interaction since we estimate the distance between these two protons to be >4.0 Å. In addition, NOESY cross-peaks (Fig. 6 and Table 4) between H-1 of **A** and H-2 and H-3 of **N** indicate that the residue corresponding to **A** is attached to β-L-Rhap **N**. This result does not unambiguously establish the linkage point, but is consistent with previous studies showing that the AceA*f* residue of RG-II is attached to a L-Rha*p* residue via a $(1\rightarrow3)$ linkage [17]. The relatively large coupling constant ($^3J_{1,2} =$ 5.0 Hz) for **A** is consistent with the cis configuration for H-1 and H-2, which in this case corresponds to the α-configuration. Thus, spin system **A** is assigned as H-1 and H-2 of an α-L-Ace*f*A residue attached to L-Rha*p* residue **N** via a $(1\rightarrow3)$ linkage (see Fig. 8). These results suggest that the previously proposed β-$(1\rightarrow3)$ linkage between Ace*f*A and L-Rhap [17] should be revised.

Spin systems **R** and **S** were assigned as β-D-Gal*p* residues, based on the chemical shifts and scalar coupling patterns of their H-1/H-4 resonances (Table 2). The COSY and TOCSY spectra, as expected for galactopyranosyl residues, contained no cross-peaks arising from the scalar coupling between H-4 and H-5 in these spin systems. The Gal*p* residue attached to O-2 of the aceric acid residue of RG-II has been proposed, on limited NMR evidence, to have the α-conformation [17]. However, no spin system corresponding to an α-D-Gal*p* residue was observed in the NMR spectra of AT-F2-VI. A cross-peak correlating H-1 of **S** and H-2 of **A** in the NOESY spectrum indicates that D-Gal*p* residue **S** is attached to aceric acid via a β-$(1\rightarrow2)$ linkage (see Fig. 8). These results suggest that the previously proposed α-$(1\rightarrow2)$ linkage between these two residues [17] should be revised.

The structure of the arabinosyl-containing side chain of AT-F2-VI. The AT-F2-VI oligosaccharides contain the unusual sugar 3-deoxy-D-*lyxo*-heptulosaric acid (Dha*p*A). The characteristic chemical shifts (δ 1.846 and 2.249) and coupling constants (Table 3) of the H-3_{ax} and H-3_{eq} resonances of a Dha*p*A residue provide a convenient starting point for tracing its spin system in COSY and TOCSY spectra. Dha*p*A was identified with spin system **O** by this criterion. The H-4 and H-5 resonances of **O** were identified in cross sections through H-3_{ax} and H-3_{eq} of this system. These cross sections did not include H-6, because of the small value of $^3J_{5,6}$. However, cross-peaks correlating H-6 with both H-4 and H-5 in the NOESY spectrum (Fig. 6 and Table 4) allowed H-6 of **O** to be identified. The chemical shifts of H-3_{ax} and H-3_{eq} of Dha*p*A (**O**) differ by 0.4 ppm, which is consistent with the previously proposed β-configuration for this residue [22]. No information regarding the specific attachment point of the Dha*p*A residue to the oligogalacturonan backbone was obtained by NMR analysis of

AT-F2-VI. However, Dha*p*A has been shown to be linked to an α-D-Gal*p*A residue via a β-(1→3) linkage in the backbone of RG-II [22].

Spin system **M** was identified as a β-L-Ara*f* residue, based on the scalar coupling pattern and chemical shifts of its six proton resonances (Table 2). The H-1, H-2 and H-3 resonances of **M** exhibit coupling patterns that may be mistaken for an α-D-Gal*p* residue. However H-4 of **M** is split by additional couplings to H-5_a and H-5_b, which would not occur in an α-D-Gal*p* residue. The fact that all six resonances of spin system **M** are observed in the TOCSY cross section taken through H-1 indicates that this system cannot represent an α-D-Gal*p* residue, in which the observed $^1H-^1H$ scalar connectivities are not expected to extend beyond H-4. The $^3J_{1,2}$ coupling (4.8 Hz) for **M** is relatively large for a furanosyl residue, consistent with the 1,2-cis configuration, which corresponds to the β-configuration in this case. The presence of a β-L-Ara*f* residue in AT-F2-VI is not surprising, as the disaccharide β-L-Ara*f*-(1→5)-D-Dha*p*A has been isolated from RG-II and rigorously characterized [19]. A strong cross-peak correlating H-1 of **M** to H-5 of **O** in the NOESY spectrum of N6H (Fig. 6 and Table 4) confirms the β-(1→5) linkage between the Ara*f* and Dha*p*A residues.

Glycosyl-linkage composition of Fraction AT-F2-VI.—The results of 1D and 2D ^1H NMR spectroscopic analysis provide evidence that Fraction AT-F2-VI contains at least two structurally related oligosaccharides in the ratio 6:1. The backbone of these oligosaccharides is composed of five (1→4)-linked α-D-Gal*p*A residues and a (1→3)-linked galactonate. The Gal*p*A residue adjacent to the terminal non-reducing Gal*p*A residue is substituted at C-2 with the apiosyl-containing side chain. The location of the Ara-(1→5)-Dha side chain residue was not established by ^1H NMR spectroscopy.

The results of glycosyl linkage composition analysis of Fraction AT-F2-VI (Table 6) are consistent with the presence of oligosaccharides containing a backbone of (1→4)-linked Gal*p*A residues that is terminated at the former reducing end with a (1→3)-linked galactonate. The data also provide evidence that a (1→4)-linked Gal*p*A residue is branched at O-2. The presence of a (1→3)-linked Gal*p*A suggests that in one oligosaccharide the Dha*p*A is attached to O-3 of the Gal*p*A residue at the non-reducing end of the backbone. In contrast, the presence of terminal non-reducing and (3,4)-linked Gal*p*A suggest that in the second oligosaccharide the Dha*p*A residue is linked to O-3 of a (1→3)-linked GalpA residue.

4. Discussion

We have provided evidence that Fraction AT-F2-VI contains at least one major and one minor structurally related oligosaccharide. In the quantitatively major oligosaccharide the (1→4)-linked Gal*p*A residue (**C** in Fig. 8) adjacent to the non-reducing end Gal*p*A residue (**G** in Fig. 8) is substituted with an aceryl acid-containing oligosaccharide side chain. The backbone of this oligosaccharide is terminated at the former reducing end with (1→3)-linked L-galactonate. This aldonic acid was generated by $NaBH_4$-reduction of the reducing (1→4)-linked Gal*p*A in the RG-II backbone prior to enzymic fragmentation. Thus, we conclude that the aceryl acid-containing side chain of RG-II (B in Fig. 1) is

Table 6
Glycosyl-linkage composition of Fraction AT-F2-VI

Glycosyl linkage	Molar ratio [a]
T-Ara*f*	0.5
4-Gal*p*	0.5
T-Gal*p*	0.1
2-Ace*f*A	0.6
3-Rha*p*	1.0
3′-Api*f*	1.0
T-Gal*p*A	0.4
2,4-Gal*p*A	1.3
3,4-Gal*p*A	0.5
4-Gal*p*A	2.4
3-Gal*p*A	0.7
3-Galactonic acid [b]	0.3

[a] Molar ratio relative to 3′Api*f* = 1.0.

[b] (1→3)-Linked galactonic acid is the expected product that results from the reduction of a (1→4)-linked reducing Gal*p*A with $NaBH_4$.

most likely located four residues in from the reducing end of RG-II.

The data obtained in this study did not provide unambiguous evidence for the location of the β-L-Araf-(1→5)-β-D-Dha*p* side chain. However, the results of NMR spectroscopic analysis and glycosyl-linkage composition analysis when taken together are consistent with the presence of at least two structurally related oligosaccharides that may differ only in the location of the Dha*p*A-containing side chain.

Prior to treatment with hot aqueous acetic acid, Fraction F2-VI was shown by ESMS analysis to contain two structurally related oligosaccharides that differed only in the presence or absence of a Kdo*p*A residue (see Fig. 3). Both oligosaccharides also contained the Dha*p*A- and aceric acid-containing side chains. Thus, we conclude that three of the four side chains (B, C, and D in Fig. 1) in RG-II must be confined to the five (1→4)-linked Gal*p*A residues closest to the reducing end of the molecule.

High-field NMR spectroscopy has the potential to solve both the primary structure and solution conformation(s) of RG-II. However, a prerequisite for such analyses is that all of the proton and carbon signals are unambiguously assigned to the appropriate glycosyl residue and that the nature of the anomeric linkages of all the glycosyl residue are established with certainty. Previous studies of chemically generated aceryl acid-containing fragments of RG-II led to the suggestion that the aceryl acid and galactosyl residues were β- and α-linked, respectively [17]. However, the results of our studies have shown that the enzymically generated aceryl acid-containing oligosaccharide contains an α-linked aceryl acid residue and a β-linked galactosyl residue. Thus, the anomeric linkages of these residues in RG-II should be revised.

The data obtained in this study do not allow us to distinguish between the two models proposed for the distribution of side chains on the RG-II backbone [23]. Nevertheless, our data do provide strong evidence for the location of the aceryl acid-containing side chain and the likely distribution of the Dha*p*A- and Kdo*p*A-containing side chains. Further NMR spectroscopic studies of RG-II and its oligosaccharide fragments will undoubtedly lead to a complete description of the primary structure of this complex pectic polysaccharide.

Acknowledgements

This work was supported in part by US Department of Energy grants DE-FG02-96ER20220 and DE-FG05-93ER20097, and by Hercules Inc., Wilmington, DE.

References

[1] A.G. Darvill, M. McNeil, P. Albersheim, *Plant Physiol.*, 62 (1978) 418–422.
[2] R.J. Redgwell, *Carbohydr. Res.*, 182 (1988) 241–258.
[3] T. Matoh, K. Ishigaki, K. Ohno, J. Azuma, *Plant Cell Physiol.*, 34 (1993) 639–642.
[4] T. Doco, P. Williams, S. Vidal, P. Pellerin, *Carbohydr. Res.*, 297 (1997) 181–186.
[5] J.R. Thomas, A.G. Darvill, P. Albersheim, *Carbohydr. Res.*, 185 (1989) 261–277.
[6] T. Matoh, S. Kawaguchi, M. Kobayashi, *Plant Cell Physiol.*, 37 (1996) 636–640.
[7] M.A. O'Neill, D. Warrenfeltz, K. Kates, P. Pellerin, T. Doco, A.G. Darvill, P. Albersheim, *J. Biol. Chem.*, 271 (1996) 22923–22930.
[8] M. Kobayashi, T. Matoh, J.-L. Azuma, *Plant Physiol.*, 110 (1996) 1017–1020.
[9] P. Albersheim, A.G. Darvill, M.A. O'Neill, H.A. Schols, A.G.J. Voragen, in J. Visser, A.G.J. Voragen (Eds.), *Progress in Biotechnology*, *Pectins and Pectinases*, Elsevier, Amsterdam, 1996, pp. 47–55.
[10] T. Ishii, T. Matsunaga, P. Pellerin, M.A. O'Neill, A.G. Darvill, P. Albersheim, *J. Biol. Chem.*, 274 (1999) 13098–13104.
[11] A. Fleisher, M.A. O'Neill, R. Ehwald, *Plant Physiol.*, 121 (1999) 829–838.
[12] M. Kobayashi, H. Nakagawa, T. Asaka, T. Matoh, *Plant Physiol.*, 119 (1999) 199–204.
[13] J. Szpunar, P. Pellerin, A. Makarov, T. Doco, P. Williams, B. Medina, R. Lobinski, *J. Anal. Atomic Spectrom.*, 13 (1998) 749–754.
[14] P. Pellerin, M.A. O'Neill, C. Pierre, M.T. Cabanis, A.G. Darvill, P. Albersheim, M. Moutounet, *J. Int. Sci. Vigne Vin.*, (1997) 33–41.
[15] M. Tahiri, P. Pellerin, J.C. Tressol, T. Doco, D. Pépin, Y. Rayssiguier, C. Coudray, *J. Nutr.*, 130 (2000) 249–253.
[16] K.S. Shin, H. Kiyohara, T. Matsumoto, H. Yamada, *Carbohydr. Res.*, 300 (1997) 239–249.
[17] M.W. Spellman, M. McNeil, A.G. Darvill, P. Albersheim, A. Dell, *Carbohydr. Res.*, 122 (1983) 131–153.
[18] L.D. Melton, M. McNeil, A.G. Darvill, P. Albersheim, *Carbohydr. Res.*, 146 (1986) 279–305.
[19] W.S. York, A.G. Darvill, M. McNeil, P. Albersheim, *Carbohydr. Res.*, 138 (1985) 109–126.

[20] T.T. Stevenson, A.G. Darvill, P. Albersheim, *Carbohydr. Res.*, 179 (1988) 269–288.
[21] T.T. Stevenson, A.G. Darvill, P. Albersheim, *Carbohydr. Res.*, 182 (1988) 207–226.
[22] V. Puvanesarajah, A.G. Darvill, P. Albersheim, *Carbohydr. Res.*, 218 (1991) 211–222.
[23] C. Hervé du Penhoat, C. Gey, P. Pellerin, S. Perez, *J Biolmol. NMR*, 14 (1999) 253–271.
[24] T. Doco, J.-M. Brillouet, *Carbohydr. Res.*, 243 (1993) 333–343.
[25] S. Vidal, J.-M. Salmon, P. Williams, P. Pellerin, *Enzyme Microbial Technol.*, 24 (1999) 283–290.
[26] P. Pellerin, T. Doco, S. Vidal, P. Williams, J-M. Brillouet, M.A. O'Neill, *Carbohydr. Res.*, 290 (1996) 183–197.
[27] T. Doco, N. Quellec, M. Moutounet, P. Pellerin, *Am. J. Enol. Vitic.*, 50 (1999) 25–32.
[28] A.J. Whitcombe, M.A. O'Neill, W. Steffan, P. Albersheim, A.G. Darvill, *Carbohydr. Res.*, 271 (1995) 15–29.
[29] A. Bax, R. Freeman, *J. Magn. Reson.*, 44 (1981) 542–561.
[30] A. Bax, D.G. Davis, *J. Magn. Reson.*, 65 (1985) 355–360.
[31] D.J. States, R.A. Haberkorn, D.J. Ruben, *J. Magn. Reson.*, 48 (1982) 286–292.
[32] G. Bodenhausen, D.J. Ruben, *Chem. Phys. Lett.*, 69 (1980) 185–189.
[33] J. Keeler, R.T. Clowes, A.L. Davis, E.D. Laue, *Methods Enzymol.*, 239 (1994) 145–207.
[34] E.R. Morris, D.A Powell, M.J. Gidley, D.A. Rees, *J. Mol. Biol.*, 155 (1982) 507–516.
[35] S.J. Angyal, *Carbohydr. Res.*, 77 (1979) 37–50.
[36] T. Ishii, M. Yamagisawa, *Carbohydr. Res.*, 313 (1998) 189–192.
[37] K. Bock, I. Lundt, C. Pedersen, *Tetrahedron Lett.*, 13 (1973) 1037–1040.